arXiv:1512.05892v1 [cond-mat.stat-mech] 18 Dec 2015

The three-dimensional $O(n)$ ϕ^4 model on a strip with free boundary conditions: exact results for a nontrivial dimensional crossover in the limit $n \to \infty$*

H. W. Diehl and Sergei B. Rutkevich
Fakultät für Physik, Universität Duisburg-Essen,
D-47058 Duisburg, Germany

December 21, 2015

Abstract

Recent exact $n \to \infty$ results for critical Casimir forces of the $O(n)$ ϕ^4 model on a three-dimensional strip bounded by two planar free surfaces at a distance L are surveyed. This model has long-range order below the bulk critical temperature T_c if $L = \infty$, but remains disordered for all $T > 0$ when $L < \infty$. A proper analysis of its scaling behavior near T_c is quite challenging: Besides with bulk, boundary, and finite-size critical behaviors, one must deal with a nontrivial dimensional crossover. The model can be solved exactly in the limit $n \to \infty$ in terms of the eigenvalues and eigenenergies of a self-consistent Schrödinger equation involving a potential $v(z)$ with the near-boundary singular behavior $v(z \to 0+) \approx -1/(4z^2) + 4m/(\pi^2 z)$, where $m = 1/\xi_+(|t|)$ is the inverse bulk correlation length and $t \sim (T - T_c)/T_c$, and a corresponding singularity at the second boundary plane. The potential $v(z)$, the excess free energy, and the Casimir force have been determined numerically with high precision. Exact analytical results for a variety of properties such as series expansion coefficients of $v(z)$, the scattering data of $v(z)$ in the semi-infinite case

*Invited talk at MQFT15

$L = \infty$ for all $m \gtrless 0$, and the low-temperature asymptotic behavior of the residual free energy and the Casimir force can be obtained by a combination of boundary-operator and short-distance expansions, proper extensions of inverse scattering theory, new trace formulae, and semiclassical expansions.

1 Introduction

Neutral atoms such as ^{4}He interact via long-range interactions — the familiar van-der-Waals interactions. Their origin is well understood (see, e.g., Ref. [1]). Owing to quantum mechanical charge fluctuations, either atom has a fluctuating dipole moment producing an electric field that the respective other one experiences. Although the averages of the dipole moments are zero, those of the squares are nonzero, as a consequence of which a fluctuation-induced (van-der-Waals) interaction results. Casimir showed in 1948 that analogous fluctuation-induced interactions occur between macroscopic metallic objects in empty space due to the disturbance of the electromagnetic ground-state energy by these objects [2]. Considering a pair of parallel grounded metallic plates of surface area A at a separation L in vacuum, he found that the (unmeasurable, infinite) electromagnetic vacuum energy per surface area A ($\to \infty$) aquires an ultraviolet finite L-dependent change

$$\Delta E_0/A = \frac{\hbar c}{2}\left[\int \frac{\mathrm{d}^2 p}{(2\pi)^2} \sum_{k,\lambda} \sqrt{p^2+k^2} - 2\int \frac{\mathrm{d}^3 q}{(2\pi)^3}\, q\right] = -\frac{\pi^2}{720}\,\frac{\hbar c}{L}\,\frac{1}{L^2}. \quad (1)$$

Here $(\boldsymbol{p}, k)$ and $\boldsymbol{q}$ are three-dimensional wavevectors; $\boldsymbol{p}$ and k are the two-dimensional and one-dimensional components parallel and perpendicular to the plates, respectively. The boundary conditions that the electromagnetic fields must satisfy on the plates imply that k is quantized, taking the values $k = \nu\pi/L$, $\nu = 0, 1, 2 \ldots$. The sum $\sum_\lambda$ runs over one or two polarizations depending on whether $\nu = 0$ or $\nu > 0$.

The form of the result is easily understood: The factor $\hbar c/L$ gives us an energy scale. Thus, dimensional considerations imply that the change of the ground-state energy per area must be of the form $\Delta E_0/A = \Delta_{\mathrm{C}}\, \hbar c L^{-3}$, where Δ_{C} is a pure number, called Casimir amplitude. This amplitude is independent of microscopic details, i.e., universal. The associated Casimir

force per area becomes

$$\mathcal{F}_C(L)/A = -\frac{\partial E_0/A}{\partial L} = -\frac{\pi^2}{240}\,\frac{\hbar c}{L^4} = -\frac{0.013001255\ldots}{(L/\mu\mathrm{m})^4}\,\frac{\mathrm{dyn}}{\mathrm{cm}^2}. \qquad (2)$$

This force depends on gross features such as the space dimension (2), the dispersion relation for electromagnetic waves and geometry. It is tiny unless the separation drops below microns. Since in micromechanical and microelectromechanical devices such small separations are realized, such Casimir forces should be taken into account and are of technological interest [3]. The reader may find an extensive account of the theory and measurements of Casimir forces and a list of references in [4].

Thirty years after Casimir's pioneering work [2], Fisher and de Gennes pointed out in a seminal paper [5] that analogous effective forces can be generated by long-wavelength, low-energy classical thermal fluctuations of systems near critical points between macroscopic objects immersed into them such as plates and container walls. The subject of such critical Casimir forces has attracted considerable attention during the last 25 years. Early attempts to detect such forces focused on their indirect confirmation through their effects on wetting layers [6, 7, 8, 9, 10]. Subsequently, Bechinger's group accomplished direct measurements of critical Casimir forces between a wall and colloidal particles immersed into binary fluid mixtures near their consolute points [11, 12, 13].

Just as the Casimir forces of QED (QEDCF), critical Casimir forces (CCF) exhibit universal properties. They depend on gross features of the medium that mediates them, namely, the universality class of the associated bulk critical behavior, on gross features of the immersed macroscopic objects or walls, which usually are encoded in the large-scale boundary conditions of the continuum field theory, and geometry. Despite obvious analogies between QEDCF and CCF, there are a number of crucial differences between them. Though pointed out previously (see, e.g., [14, 15, 16, 17]), these differences are not always fully appreciated. A first obvious difference is that CCF originate from thermal rather than quantum fluctuations. Quantum fluctuations do not contribute to the leading large-distance asymptotic behaviors unless one is dealing with fluctuation-induced forces near quantum critical points [18].

A second important difference is the following: The universal properties of QEDCF can normally be modeled by effective free field theory in which interaction of the electromagnetic fields with macroscopic objects such as

metallic plates are taken into account via boundary conditions. In the case of CCF, one usually must deal with interacting classical field theories such as ϕ^4 theories. This is dictated by the requirement that the bulk critical behavior is properly described.

A further difference is that unlike QEDCF, CCF are not normally fully fluctuation induced. The reason is that the order parameter ϕ may acquire a nonzero average in a strip geometry — either in the low-temperature regime (if the system has long-range order) or even generically at all temperatures as in the case of classical fluids and binary fluid mixtures owing to the explicit breaking of the $\phi \to -\phi$ symmetry by boundary fields [19, 20]. If $\langle\phi\rangle \neq 0$, then this average will react to changes of the separation between boundary planes, producing thereby an effective force even in Landau theory. If so, the CCF consists of a non-fluctuating background plus fluctuation-induced contributions.

In the present paper we shall focus on the case of CCF in systems whose critical behavior can be described by an $O(n)$ invariant Hamiltonian. Our interest in this problem derives from several sources. First of all, the $O(2)$ case is of direct relevance for experiments that measure CCF in ^{4}He near the superfluid λ transition via the thinning of wetting layers [6, 8]. Second, we believe that this problem represents a much closer analog to QEDCF than that of binary fluid mixtures. This is because the order-parameter profile $\langle\phi(\boldsymbol{r})\rangle$ of ^{4}He remains zero for all temperatures $T > 0$ whenever the thickness L of the strip is finite. Third, we consider this challenging problem to be of fundamental importance. What makes it quite hard is that it involves difficulties beyond those usually encountered in studies of CCF in systems with free boundaries, namely, the requirement to simultaneously treat bulk, boundary, and finite-size critical behaviors. The additional complication one must cope with in the case of three-dimensional strips with $O(n)$ symmetric Hamiltonian is the subtle dimensional crossover of a three-dimensional bulk ($L = \infty$) system with long-range order (LRO) at low temperatures to an $L < \infty$ strip with no LRO at any $T > 0$ [16, 17, 21].

The purpose of the present paper is to elucidate these problems and show how they can all be handled within one and the same approach, namely, the exact solution for $n \to \infty$. We will explain why the $n = \infty$ solutions for the scaling functions of the residual free energy and the CCF under free boundary conditions (fbc) are considerably harder to obtain than their analogs under periodic boundary conditions (pbc) and that the behaviors of the former differ qualitatively and quantitatively from those of the latter.

The remainder of this paper is organized as follows. In the next section, we introduce the $O(n)$ ϕ^4 model on a strip, specify the boundary conditions, and discuss its finite-size phase diagram. We then recall that the model can be solved exactly in the $n \to \infty$ solution in terms of the eigenvalues and eigenstates of a selfconsistent one-dimensional Schrödinger equation.

2 Model, boundary conditions, and background

2.1 Hamiltonian and boundary conditions

We consider a model defined by the reduced Hamiltonian

$$\mathcal{H}[\boldsymbol{\phi}] = \int_{\mathfrak{V}} \mathrm{d}^d r \left[\frac{1}{2}(\nabla\boldsymbol{\phi})^2 + \frac{\mathring{\tau}}{2}\phi^2 + \frac{g}{4!n}\phi^4\right] + \frac{\mathring{c}}{2}\int_{\mathfrak{B}_1\cup\mathfrak{B}_2} \mathrm{d}^{d-1} y\, \phi^2 \;, \qquad (3)$$

where $\boldsymbol{\phi}(\boldsymbol{r}) = (\phi_\alpha(\boldsymbol{r}))$, $\alpha = 1, \ldots, n$, is a real-valued n-component order-parameter field defined on the d-dimensional strip $\mathfrak{V} = \mathbb{R}^{d-1} \times [0, L]$. We write the position vector as $\boldsymbol{r} = (\boldsymbol{y}, z)$ where $\boldsymbol{y} \in \mathbb{R}^{d-1}$ and $z \in [0, L]$ are the coordinates parallel and perpendicular to the boundary planes $\mathfrak{B}_1 = \{\boldsymbol{y}, 0)\}$ and $\mathfrak{B}_2 = \{(\boldsymbol{y}, L)\}$, respectively. Here $(\nabla\boldsymbol{\phi})^2$ is a short-hand for $\sum_\alpha (\nabla\phi_\alpha)^2$ and ϕ^2 denotes the square $\sum_\alpha \phi_\alpha^2$ of the length of $\boldsymbol{\phi}$.

The boundary terms of the Hamiltonian imply the so-called Robin boundary conditions [19, 20, 15]

$$\partial_n \boldsymbol{\phi} = \mathring{c}\,\boldsymbol{\phi}, \quad \boldsymbol{r} \in \mathfrak{B}_1 \cup \mathfrak{B}_2, \qquad (4)$$

where ∂_n means the derivative along the inner normals. For simplicity, we have chosen the same value of $\mathring{c}$ on both boundary planes. Relaxing this condition by choosing different values of $\mathring{c}_j$ on $\mathfrak{B}_j$ would be straightforward [15, 14, 17, 21] but not necessary here because we shall focus on the case in which the large-distance behavior is governed by a fixed point corresponding to Dirichlet boundary conditions (DD) on both planes $\mathfrak{B}_1$ and $\mathfrak{B}_2$, which can be studied by setting $\mathring{c} = \infty$ [19, 20, 15, 14].

The model under pbc along the z-direction,

$$\boldsymbol{\phi}(\boldsymbol{y}, L) = \phi(\boldsymbol{y}, 0), \qquad (5)$$

is defined in a similar fashion; in this case the boundary term involving $\int_{\mathfrak{B}_1\cup\mathfrak{B}_2}$ in Eq. (3) is absent since there are no boundaries.

2.2 Remarks on UV singularities and renormalization issues

We will consider these models for $2 < d < 4$. Our main interest will be the case of $d = 3$ dimensions. Therefore, we shall frequently specialize to $d = 3$. For $d < 4$, these models are superrenormalizable. The ultraviolet (UV) singularities in multi-point cumulants can be absorbed in the bulk critical value $\mathring{\tau}_c$ (pbc and fbc) and an analogous special value $\mathring{c}_{\mathrm{sp}}$ (fbc) by introducing the renormalized quantities (pbc and fbc)

$$\tau = \mathring{\tau} - \mathring{\tau}_c \tag{6}$$

and (only fbc)

$$\mathring{c} = c - \mathring{c}_{\mathrm{sp}}. \tag{7}$$

If one regularizes by means of a large-momentum cutoff Λ, these shifts vary as $\mathring{\tau}_c \sim \Lambda^{d-2}$ and $\mathring{c}_{\mathrm{sp}} \sim \Lambda^{d-3}$. At $d = 4$ additional (logarithmic) UV singularities appear, which require further reparametrizations. The interested reader may find the relevant details concerning this issue and how to renormalize the theory in $4-\epsilon$ dimensions in the review articles [19, 20] and various original papers [22, 23, 24, 25, 15, 14]. Since we will restrict ourselves to the case of $2 < d < 4$, we shall not have to bother with this matter. However, bulk and surface free energies require subtractions (additive counterterms) to cancel their UV singularities even when $d < 4$. We shall restrict ourselves to occasional remarks at appropriate places and otherwise refer the reader to more detailed expositions in the literature.

2.3 Bulk, surface, excess, and residual free energies

Keeping in mind that quantities such as free energies and the partition function require a regularization of UV singularities to be well defined, we introduce the partition functions formally through the functional integral $\mathcal{Z} = \int \mathcal{D}[\boldsymbol{\phi}]\, e^{-\mathcal{H}[\boldsymbol{\phi}]}$ and the reduced free energy $-A^{-1}n^{-1}\ln\mathcal{Z}$ per surface area $A = \int \mathrm{d}^{d-1}y \to \infty$ and number of components. We can then define the limit $n \to \infty$ of the free energy (area) density f_L, the bulk free energy density f_{b}, the excess free energy density f_{ex}, the surface free energy f_{s}, and

the residual free energy $f_{\rm res}$ through

$$
\begin{aligned}
f_L &= -\lim_{n\to\infty}\lim_{A\to\infty}\frac{\ln\mathcal{Z}}{nA}\,, && (8)\\
f_{\rm b} &= \lim_{L\to\infty} f_L/L, && (9)\\
f_{\rm ex}(L) &\equiv f_L - L\,f_{\rm b}, && (10)\\
f_{\rm s} &= f_{\rm ex}(\infty)/2, && (11)\\
f_{\rm res}(L) &= f_{\rm ex}(L) - 2f_{\rm s}. && (12)
\end{aligned}
$$

The bulk free energy $f_{\rm b}$ is independent of the boundary conditions (pbc or fbc). The other four free energies differ for fbc and pbc. Specifically, $f_{\rm s}^{\rm fbc}$, $f_{\rm ex}^{\rm fbc}$, and $f_{\rm res}^{\rm fbc}(L)$ depend also on the surface interaction constant $\mathring{c}$, while $f_{\rm s}^{\rm pbc}\equiv 0$.

2.4 Finite-size phase diagram for $d = 3$

The Hamiltonian (3) of the $O(n)$ ϕ^4 theory is invariant under the continuous $O(n)$ symmetry. According to the Mermin-Wagner theorem [26], such a symmetry cannot be spontaneously broken at any temperature $T > 0$ in bulk systems with short-range interactions if $d \le 2$. However, for $d > 2$ a phase with long-range bulk order (bulk LRO) exists below a critical temperature $T_{\rm c} > 0$. Rigorous extensions of the Mermin-Wagner theorem imply that classical ferromagnetic $O(n)$ models on networks cannot have a spontaneous magnetization at any $T > 0$ if random walks on the same structure are recurrent, i.e., return to their starting point with probability one [27]. Since random walks in a three-dimensional rectangular cuboid of cross-sectional area $A = \infty$ and finite thickness L are recurrent, no LRO phase is possible for $d = 3$ at any $T > 0$ when $L < \infty$. At $d = 3$ we therefore have the finite-size phase diagram displayed in Fig. 1, irrespective of whether we choose prb or fbc.

The LRO low-temperature and disordered high-temperature bulk phases are located on the line $1/L = 0$. As temperature variable we have introduced

$$
m = \mathrm{sgn}(t)/\xi_{\rm b}(|t|) \simeq \mathrm{sgn}(t)\,|t|^{\nu}/\xi_{\rm b}^{(+)}, \qquad (13)
$$

where $\xi_{\rm b}^{(+)}$ is the amplitude of the bulk correlation length $\xi_{\rm b} \simeq \xi_{\rm b}^{(+)}\,t^{\nu}$ in the disordered ($t > 0$) phase and $\nu = (d-2)^{-1}|_{d=3} = 1$ for $n = \infty$. The lines $L^{-1} = \pm m$ are finite-size crossover lines: on scales $|m|^{-1} \gtrsim L$, the

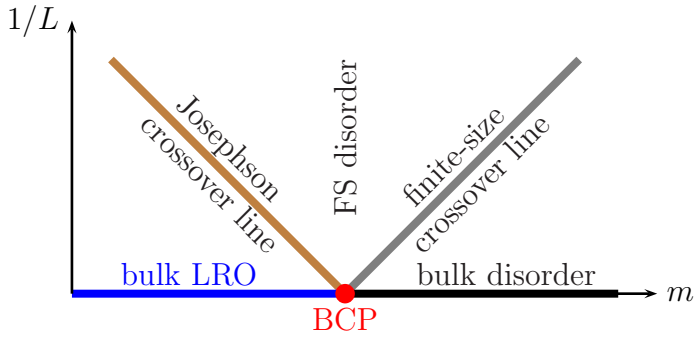

Figure 1: Finite-size phase diagram for $d = 3$. The bulk critical point (BCP) separates the low-temperature phase with bulk LRO from the disordered high-temperature bulk phase. The lines $L = \pm|m|$ are crossover lines. For further explanation see main text.

system does not longer exhibit 3D bulk behavior but becomes effectively 2D. In the case of fbc, where the translation invariance along the z-direction is broken, the length $|m|^{-1}$ also characterizes the thickness of the boundary regions within which local densities deviate for $z \lesssim |m|^{-1} << L/2$ and $L - z \lesssim |m|^{-1} \ll L$ from their bulk values, which they approach in the limits $z, L \to \infty$ with $z < L$, and $L - z, L \to \infty$ with $L - z < L/2$. The approach to bulk behavior is exponential in L when $m > 0$. Thus, in the case of fbc, the deviations of local densities from their bulk values vary as $\sim \exp[-2zm + \mathrm{O}(\ln zm)]$ as $z, L \to \infty$ with $0 < m^{-1} \ll z \ll L/2$. Likewise, excess quantities which vanish in the limit $L \to \infty$ such as f_{ex} decay for fbc as $\exp[-2mL + \mathrm{O}(\ln mL)]$ at large L. The factor of 2 in both exponential forms can be understood via perturbation theory: the disturbance caused by the presence of a free surface at $z = 0$ gives contributions to the free two-point function that depend on the distance $2z$ of one of its points $\boldsymbol{r} = (\boldsymbol{y}, z)$ from the image point $(\boldsymbol{y}, -z)$. In the case of pbc (no boundaries), one has $f_{\mathrm{ex}} \sim \exp[-mL + \mathrm{O}(\ln mL)]$ instead.

For $m < 0$, there is LRO in the bulk when $d \geq 3$. Owing to the spontaneous breaking of the $O(n)$ symmetry, correlations decay algebraically rather than exponentially fast, so that usual moment-based definitions of a correlation length are inapplicable [28]. An appropriate coherence length or helicity

length $\xi_{\rm hel}$ characterizing the asymptotic decay of the bulk correlation function $\langle \boldsymbol{\phi}(\boldsymbol{r}) \cdot \boldsymbol{\phi}(\boldsymbol{0}) \rangle$ can be defined in terms of the familiar helicity modulus $\Upsilon(T)$ through $\xi_{\rm hel} = [(k_{\rm B}T/\Upsilon(T)]^{1/(d-2)}$. Since $\Upsilon \sim |m|^{\nu(d-2)}$ as $m \to 0-$ for $2 < d < 4$, this helicity length (or Josephson coherence length) varies as $\xi_{\rm hel} \sim |m|^{-\nu}$ in this limit, with $\nu|_{n=\infty} = (d-2)^{-1}$. Specifically at $d = 3$, the temperature variable $|m|$ corresponds to $1/\xi_{\rm hel}$ (up to a normalization factor).

The length $\xi_{\rm hel}$ plays a role analogous to ξ_+ for $t > 0$: When it becomes comparable to L, finite-size corrections become important, and in the case of fbc, it characterizes the thickness of the boundary regions $z \lesssim \xi_{\rm hel} \ll L$ and $L - z \lesssim \xi_{\rm hel} \ll L$.

3 Exact $n \to \infty$ solution of the model

3.1 selfconsistent equations at $n = \infty$

There are different ways to derive the equations that must be solved to obtain the exact $n \to \infty$ solution of our model (see, e.g., Refs. [29, 30]). One possibility is to use the Hubbard-Stratonovich transformation

$$\exp\Big[-\frac{g}{4!n}\phi^4\Big] \propto \int_{-\infty}^{\infty} \mathrm{d}\psi \exp\Big[\frac{1}{2}\phi^2\,\mathrm{i}\psi - \frac{3n}{2g}\,\psi^2\Big] \tag{14}$$

to conclude that the model in the large-n limit is equivalent to n copies of a constrained Gaussian model with a one-component field $\Phi(\boldsymbol{r})$ (representing anyone of the components ϕ_α), where the boundary conditions (4) or (5) must be taken into account. This Gaussian model has the effective Hamiltonian

$$\mathcal{H}_{\rm eff}[\Phi,\psi] = \frac{1}{2}\int_{\mathfrak{V}} \mathrm{d}^d r \Big[\Phi\left(-\nabla^2 + \mathring{\tau} + \mathrm{i}\psi\right)\Phi + \frac{3n}{g}\psi^2\Big], \tag{15}$$

where $\psi(\boldsymbol{r})$ is an auxiliary field. In the limit $n \to \infty$, the ψ-integration reduces to the value of the integrand at the saddle point. Unlike the case of pbc, this saddle point is z-dependent owing to the breakdown of translation invariance along the z-direction. Writing it as

$$\mathrm{i}\psi(z) = v(z) - \mathring{\tau}, \tag{16}$$

one finds that the free energy f_L can be expressed as

$$f_L = \frac{1}{2}\int_{\boldsymbol{p}}^{(d-1)} \sum_{\nu} \ln(p^2 + \varepsilon_\nu) - \frac{3}{2g}\int_0^L \mathrm{d}z\,[\mathring{\tau} - v(z)]^2 \tag{17}$$

in terms of the eigenvalues ε_ν and eigenfunctions $\varphi_\nu(z)$, $\nu = 1, 2, \ldots$, of the selfconsistent Schrödinger equation defined by

$$[-\partial_z^2 + v(z)]\varphi_\nu(z) = \varepsilon_\nu\, \varphi_\nu(z) \tag{18}$$

and the self-consistency condition

$$\mathring{\tau} - v(z) = \bigcirc\!\!\!\!\!\!\bullet = -\frac{g}{6} \int_{\boldsymbol{p}}^{(d-1)} \sum_\nu \frac{|\varphi_\nu(z)|^2}{\boldsymbol{p}^2 + \varepsilon_\nu}, \tag{19}$$

where $\boldsymbol{p} \in \mathbb{R}^{d-1}$ is the wavevector conjugate to $\boldsymbol{y}$.

In writing these equations, we have tacitly assumed the absence of any LRO, so that $\langle \Phi(\boldsymbol{r}) \rangle = 0$. In the semi-infinite case, $L = \infty$, LRO would occur for $d > 2$ whenever $\mathring{\tau}$ falls below its bulk critical value $\mathring{\tau}_c = -(g/6) \int_{\boldsymbol{q}}^{(d)} q^{-2}$. However, for $d > 3$, the surface can order for $\mathring{\tau} > \mathring{\tau}_c$ provided $\mathring{c}$ exceeds a negative threshold value $\mathring{c}_{\rm sp}$. We will not consider the latter case, assuming $\mathring{c}$ to be sufficiently large so that the order-parameter profile $\langle \Phi(\boldsymbol{r}) \rangle$ vanishes for all values of $\mathring{\tau}$ and for all $\mathring{\tau} \geq \mathring{\tau}_c$ depending on whether $L < \infty$ and $L = \infty$, respectively.

3.2 Scaling forms

We are interested in the long-length-scale (scaling) solutions of Eq. (19) both for pbc and fbc, and wish to exploit them to determine the scaling forms of the residual free energy $f_{\rm res}$ and the Casimir force $\mathcal{F}_C$ for $L \to \infty$ and $m \to 0$ at fixed $x \equiv mL$. Since the potential $v(z)$ corresponds to the energy density which scales as $m^{d-1/\nu} \underset{n=\infty}{=} m^2$, we have

$$v(z; L, m) = m^2\, v(|m|z; |m|L, \pm 1) = \frac{v(z/L; 1, mL)}{L^2} = \frac{v(1; L/z, mz)}{z^2} \tag{20}$$

for fbc. For pbc, the z-dependence drops out so that only the first two equations prevail, with the first (z-related) arguments of the vs omitted.

The residual free energy and the Casimir force take the scaling forms

$$\begin{aligned} f_{\rm res}(L, m) &\simeq L^{-(d-1)}\, \Theta(mL)\,, \\ \mathcal{F}_C(L, m) &\simeq L^{-d}\, \vartheta(mL), \end{aligned} \tag{21}$$

with

$$\vartheta_d(x) = (d-1)\, \Theta_d(x) - x\, \Theta_d'(x), \tag{22}$$

where Θ and ϑ are universal functions depending on d and the boundary conditions.

3.3 Exact $n = \infty$ results for periodic boundary conditions

The z-independence of the potential $v^{\rm pbc}(L,m)$ for pbc implies that the corresponding eigenvalues and eigenfunctions are explicitly known: we have $\varepsilon_\nu^{\rm pbc} = v^{\rm pbc} + k_\nu^2$ and $\varphi_\nu^{\rm pbc}(z;L,m) = L^{-1/2}\, e^{{\rm i}k_\nu z}$ with $k_\nu = 2\pi\nu/L$. Specifically at $d=3$, the scaled potential and the scaling functions can be determined in closed form [31, 32, 33]. One finds

$$\check{v}(x) \equiv v^{\rm pbc}(L=1, m=x) \underset{d=3}{=} \big[2\,\mathrm{arcsinh}\big(e^x/2\big)\big]^2 \tag{23}$$

and

$$\Theta(x) \underset{d=3}{=} -\frac{8\pi^2 x^3}{3}\,\theta(x) + Q\Big[\sqrt{\check{v}(x)}\Big] - \frac{\check{v}(x)}{12\pi} + \frac{x\,\check{v}(x)}{2} \tag{24}$$

with

$$Q(y) \equiv \frac{1}{4\pi}\int_{y^2}^{\infty} {\rm d}t\, \ln\big[1 - e^{-\sqrt{t}}\big] = -\frac{1}{2\pi}\big[{\rm Li}_3(e^{-y}) + y\,{\rm Li}_2(e^{-y})\big], \tag{25}$$

where $\theta(x)$ denotes the Heaviside function and ${\rm Li}_s(x)$ is the polylogarithm. The scaling functions $\Theta^{\rm pbc}(x)$ and $\frac{1}{2}\vartheta^{\rm pbc}(x)$ for $d=3$ are shown in Fig. 2. They are negative and monotonically decreasing for all x. Their value

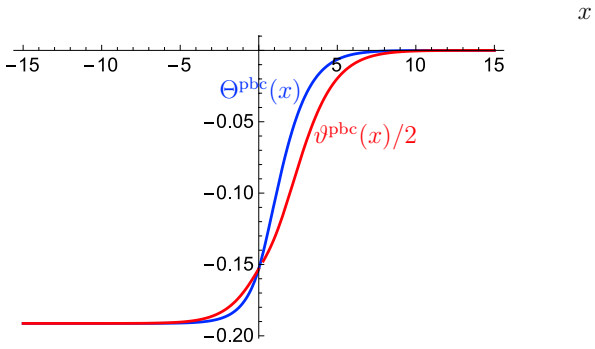

Figure 2: Scaling function $\Theta(x)$ and $\vartheta(x)/2$ for $(d,n) = (3,\infty)$ and periodic boundary conditions.

$$\Delta_C^{\rm pbc} \equiv \Theta_{d=3}^{\rm pbc}(0) = \frac{1}{2}\,\vartheta_{d=3}^{\rm pbc}(0) = -\frac{2\,\zeta(3)}{5\pi} = -0.1530506\ldots \tag{26}$$

at T_c defines the so-called Casimir amplitude Δ_C. The $x \to -\infty$ saturation value

$$\Delta_{G,C}^{\rm pbc} = \Theta_{d=3}^{\rm pbc}(-\infty) = \frac{1}{2}\,\vartheta_{d=3}^{\rm pbc}(-\infty) = -\frac{\zeta(3)}{2\pi} = -0.191313298\ldots \qquad (27)$$

is the corresponding amplitude for a massless scalar free field theory.

3.4 General features of the scaling functions for free boundary conditions

The behaviors of $\Theta(x) \equiv \Theta^{\rm fbc}(x)$ and $\vartheta(x) \equiv \vartheta^{\rm fbc}(x)$ differ qualitatively and quantitatively from those of their analogs for pbc. First evidence for this fact was provided by experimental investigations of the thinning of wetting layers of ^{4}He in contact with copper substrates at and below the normal-to-superfluid λ transition [6, 8]. The scaling function $\vartheta_{^4{\rm He}}(x)$ extracted from the wetting data turned out to be negative definite for all x, just as the $n = \infty$ result $\vartheta^{\rm pbc}(x)$ shown in Fig. 2. However, unlike the latter function it did not monotonically decrease from $\vartheta(\infty) = 0$ to its limiting value $\vartheta(-\infty)$ as $x \to -\infty$, but went through a minimum located at $x < 0$ and subsequently seemed to increase monotonically to a limiting value $\vartheta(-\infty) < 0$ upon further decrease of x. This behavior could be corroborated by Monte Carlo calculations for the XY model on a $d = 3$ dimensional film with fbc along the short direction [34, 35, 36, 37]. Although these experimental and simulation results apply to the $n = 2$ case of ^{4}He, the $n = \infty$ scaling function $\vartheta^{\rm fbc}(x)$ is expected to display the same qualitative features, namely, (i) negative definiteness for all x, (ii) a pronounced smooth minimum at a value $x_{\rm min} < 0$, and a (iii) monotonic approach to a limiting value $\vartheta(-\infty) < 0$. On the other hand, the $n = 2$ (^{4}He) case is special in that a Kosterlitz-Thouless transition occurs to the left of the minimum. It has been identified by Monte Carlo simulations [38, 37], but leaves hardly any visible trace in $\vartheta_{n=2}^{\rm fbc}(x)$.

It is a major challenge to determine the scaling functions $\vartheta^{\rm fbc}(x)$ and $\Theta^{\rm fbc}(x)$ for all x within a single approximation scheme such that all of their explained important properties are obtained at least in a qualitatively correct fashion. Perturbative renormalization-group (RG) approaches based on the ϵ expansion about the upper critical dimension $d^* = 4$ have been found to give acceptable results for the disordered phase $x > 0$ [39, 40, 15, 14], but are not normally able to describe dimensional crossovers in a proper fashion.

Thus the ϵ-expansion breaks down for $L < \infty$ near the critical or pseudo-critical point of the film [14, 41, 42, 43]. In the case of pbc, Landau theory erroneously predicts a critical point of the film right at T_c. Therefore, the ϵ expansion breaks down at T_c [41]. For fbc, the film becomes critical in Landau theory at an L and $\mathring{c}$-dependent temperature $T_{c,L} < T_c$. We can set $\mathring{c} = \infty$ and choose Dirichlet boundary conditions. Then the film critical point is located at $\mathring{\tau} - \mathring{\tau}_c = -(\pi/L)^2$, where the eigenvalue ε_1 of the lowest mode vanishes.

The mean-field (Landau theory) scaling function $\vartheta_{\rm MF}^{\rm fbc}(x)$ was determined exactly in [44, 45]; it is plotted in Fig. 3. The critical temperature of the

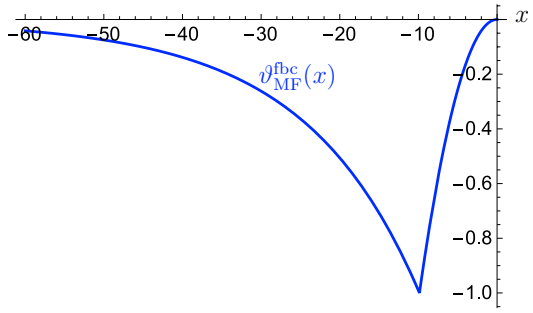

Figure 3: MF scaling function $\vartheta_{\rm MF}^{\rm fbc}(x)$ for fbc. Following [44], we have normalized its amplitude such that the minimum value at $x_{\rm min} = -\pi^2$ is -1. For $x > 0$, this function vanishes.

film, $T_{c,L}$, translates into the location of the minimum of $\vartheta_{\rm MF}^{\rm fbc}(x)$. Since the $\epsilon = 4-d$ expansion is based on an expansion about Landau theory, it is clear that it would not run into difficulties in handling the crossover to the effective $(d-1)$-dimensional long-distance behavior near $T_{c,L}$ in a proper fashion even if a critical point existed at $T > 0$ for $L < \infty$ (as it does in the $n = 1$ case). For $n \geq 2$, the situation is even worse because LRO is ruled out at $d \leq 3$ for all $T > 0$ when $L < \infty$. The MF prediction is qualitatively wrong not only in that it predicts a sharp transition at a $T_{c,L} > 0$ for $L < \infty$ when $n \geq 2$ and $d \leq 3$. Its predictions are also in conflict with other important qualitative properties of $\vartheta_{^4{\rm He}}^{\rm fbc}(x)$ mentioned above. Unlike the latter function, $\vartheta_{\rm MF}^{\rm fbc}(x)$ is not continuously differentiable near the minimum. Rather, its derivative has a jump discontinuity at $x_{\rm min}$. Furthermore, $\vartheta_{\rm MF}^{\rm fbc}(x)$ vanishes as $x \to -\infty$ instead of approaching a negative value. This is because MF theory ignores

fluctuation effects due to Goldstone modes on scales $|m|^{-1} \lesssim L$. Due to the same reason, MF theory fails to predict the absence of LRO at $T > 0$ for $L < \infty$ in the continuous symmetry case $n \geq 2$ when $d \leq 2$. By contrast, the $n \to \infty$ limit complies with the Mermin-Wagner theorem [26, 27], providing a mechanism for nonperturbative mass generation.

Unfortunately, it is not easy to obtain exact analytical information about the potential $v(z) \equiv v^{\rm fbc}(z)$ and the scaling functions $\Theta^{\rm fbc}(x)$ and $\vartheta^{\rm fbc}(x)$ for general values of m and L, even at $d = 3$. The reason is that $v(z)$ depends on z. Accordingly, the spectrum $\{\varepsilon_\nu\}$ and eigenfunctions of Eq. (18) are not generally known but must be determined from Eq. (18), which must be solved selfconsistently with Eq. (19) to obtain $v(z)$. This is a rather hard problem.

The scaling solution $v(z)$ of these equations for finite L is not even known in closed analytic form at $T_{\rm c}$. To gain information about $v(z)$, distinct methods can and have been used, namely, (i) their direct solution for $m = 0$ and $L = \infty$ [46], (ii) boundary-operator (BOE) and short-distance expansions (SDE) [47], (iii) numerical solutions [16, 17, 48, 49], (iv) inverse scattering theory (IST) [21], (v) trace formulae, (vi) mapping of the model for large $-x$ to the nonlinear σ model [16, 17], and (vii) semiclassical expansions [21]. In the following, we will briefly survey the exact results obtained by these methods, focusing on the case $d = 3$ unless stated otherwise.

4 Survey of exact $n = \infty$ results for free boundary conditions

Bray and Moore [46] managed to find the exact scaling solutions for the semi-infinite critical case $(m, L) = (0, \infty)$ for $2 < d < 4$. To this end, they used the ansatz $v(z) = Az^{-2}$, solved Eq. (18) on the half-line $z \geq 0$ under the boundary condition that the eigenfunctions vary $\sim z^{1/2}$ for $z \to 0$ in terms of Bessel functions, and determined the coefficient A from the self-consistency condition (19). This gave

$$v(z;\infty,0) = \begin{cases} \frac{(d-3)^2-1}{4z^2} & \text{for } 2 < d < 4 \\ \frac{(5-d)^2-1}{4z^2} & \text{for } 3 < d < 4 \end{cases} \underset{d=3}{=} \frac{-1}{4z^2}. \tag{28}$$

The additional solution found for $3 < d < 4$ applies to the so-called "special" surface transition where the variable $\mathring{c}$ takes the above-mentioned threshold

value $\mathring{c}_{\rm sp}$ [19]. For $d = 3$ only the solution associated with the so-called "ordinary" surface transition remains. The results are in conformity with the rightmost scaling form given in Eq. (20) and show that one must deal with potentials that are singular at the boundary. Since for general values of L and m, the near-boundary behaviors for $z \to 0+$ and $z \to L-$ must comply with Eq. (28), $v(z)$ behaves singularly at either boundary plane. Specifically for $d = 3$, one must have

$$v(z; L, m) \simeq \frac{-1}{4} \begin{cases} z^{-2}, & z \to 0+, \\ (L-z)^{-2}, & z \to L-. \end{cases} \tag{29}$$

Schrödinger operators with singular potentials are somewhat subtle since the issue of whether a self-adjoint extension exists and which boundary condition must be imposed on the wave functions (see e.g. [50]). An early investigation can be found in [51, 52]. In the textbook [52], the radial Schrödinger equation a$R'' + 2/rR - v(r)R = \varepsilon R$ is discussed for the potential $-\gamma/r^2$. The value $\gamma = 1/4$, which according to Eq. (28) holds for $d = 3$ turns out to be a threshold: whereas physically meaningful self-adjoint extensions exist for $\gamma \geq 1/4$ [53, 54], this is not the case for $\gamma < 1/4$, where no acceptable energy operator bounded from below results [55].

Let us introduce different scaling functions $\mathcal{V}_\pm$ depending on whether $m \gtrless 0$, writing

$$v(z; L, m) = z^{-2}\, \mathcal{V}_\pm(z/L, |m|z). \tag{30}$$

Information about the behavior of $\mathcal{V}_\pm(\mathfrak{z}, \mathsf{z})$ for $\mathfrak{z} \to 0$ can be deduced via the BOE by exploiting the fact that the contribution from the component T_{zz} of the stress tensor yields the leading small-$\mathfrak{z}$ correction [47]. One obtains for $d = 3$,

$$\mathcal{V}_\pm(\mathfrak{z}, \mathsf{z}) \underset{\zeta \ll 1}{=} A_\pm(\mathsf{z}) + \mathfrak{z}^3\, B_\pm(\mathsf{z}) + \ldots, \tag{31}$$

where the functions $A_\pm(\mathsf{z})$ and $B_\pm(\mathsf{z})$ are known to behave as

$$A_\pm(\mathsf{z}) \underset{\mathsf{z} \ll 1}{=} -\frac{1}{4} \pm \frac{4\mathsf{z}}{\pi^2} + \frac{56\,\zeta(3)\,\mathsf{z}^2}{\pi^4} + \mathrm{o}(\mathsf{z}^2), \tag{32}$$

$$B_\pm(\mathsf{z}) \underset{\mathsf{z} \ll 1}{=} \frac{256\,\Delta_C}{\pi} + \mathrm{O}(\mathsf{z}). \tag{33}$$

The first term on the right-hand side of Eq. (32) is known from [46], the second was derived in [47] by an appropriate extension of the direct solution.

The third term was determined in [21] using IST in conjunction with a trace formula [54]. Finally, the result $B_{\pm}(0)$ given in Eq. (33) was obtained in [47] by exploiting the BOE and SDE along with results due to Cardy [56] and [57]. The exact analytical value of the Casimir amplitude it involves is not known. However, the numerical work of [16, 17] yielded the high-precision result

$$\Delta_C = -0.01077340685024782(1). \tag{34}$$

To achieve such a precision, good understanding and control of corrections to scaling was necessary. At $d = 3$, anomalous corrections $\sim L^{-1} \ln L$ appear because the bulk correction-to-scaling exponent $\omega|_{n=\infty} = 4 - d$ is degenerate with the surface correction-to-scaling exponent $d - (d - 1) = 1$ associated with the boundary operator T_{zz} [16, 17, 20, 58]. The corrections to scaling could be partly suppressed by taking the limit $g \to -\infty$, in which the model reduces to the spherical model of [49] with separate constraints on the energy density for each layer z [48]. The remaining corrections to scaling could be largely absorbed by a change of L to an effective thickness L_{eff}.

In [16, 17], Eqs. (18) and (19) were solved numerically to obtain $v(z; L, m)$, the eigenvalues ε_ν and eigenfunctions for different values of $m \gtrless 0$ and L, and then analyzed to determine the scaling functions $\Theta^{\text{fbc}}(x)$ and $\vartheta^{\text{fbc}}(x)$. The results display all important qualitative features known from the ^{4}He case. We refrain from reproducing these results here, referring the interesting reader to the original papers. Instead, we will report some additional exact results and mention how these were obtained.

One fruitful method is to use IST. Recall that IST aims at reconstructing the potential from scattering or spectral data. To become more specific, consider the semi-infinite case $L = \infty$. Let us subtract from $v(z; \infty, \pm|m|)$ its bulk value $\theta(m)\, m^2$ to obtain potentials $v(z; \infty, \pm 1) - m^2\, \theta(m)$ to arrive at potential that vanish as $z \to \infty$, and scale m to 1, introducing $\mathsf{z} = z|m|$ and the rescaled wavenumber $\mathsf{k} = \mathsf{k}/|\mathsf{m}|$. We can introduce two Jost solutions of the Sturm-Liouville equation implied by Eq. (18) with the limiting behavior $f(\mathsf{z}, \pm\mathsf{k}) \underset{\mathsf{z}\to\infty}{\simeq} \mathsf{e}^{\pm \mathrm{i}\mathsf{k}\mathsf{z}}$ and then choose a linear combination, the "regular solution," that satisfies the boundary condition $\varphi(\mathsf{z}, \mathsf{k}) = \sqrt{\mathsf{z}}\,[1 + \mathrm{O}(\mathsf{z})]$. Its asymptotic behavior

$$\varphi(\mathsf{z}, \mathsf{k}) \underset{\mathsf{z}\to\infty}{\simeq} \frac{\mathsf{A}(\mathsf{k})}{\mathsf{k}} \sin[\mathsf{k}\mathsf{z} + \eta(\mathsf{k})], \quad \mathsf{A}(\mathsf{k}) = \mathsf{e}^{\sigma(\mathsf{k})} \tag{35}$$

defines the scattering amplitude $A(\mathsf{k})$ and phase shift $\eta(\mathsf{k})$. In our case these

scattering data differ for $m = \pm 1$, which we indicate through subscripts on $A_\pm(\mathsf{k})$ and $\eta_\pm(sk)$.

Two difficulties had to be overcome to use IST. First, IST had to be generalized to potentials with singular behaviors of the form $v(\mathsf{z}) \simeq -\mathsf{z}^{-2}/4 + v_{-1}\mathsf{z}^{-1} + \mathrm{O}(1)$. Second, the scattering data are not given to reconstruct the potentials from them. We used the following trick. We introduced a free-energy function $f[v]$ whose stationary equation $\delta f[v]/\delta v(z) = 0$ yields Eqs. (19) and (18). We then considered variations $v(z) = v_*(z) + \delta v(z)$ about the stationary solution $v_*(z)$, which were chosen such that the singular part of $v(z)$ remained the same. We then expressed $\delta f[v_*, \delta v] = \int_0^\infty \mathrm{d}z\, \delta v(z)\, \delta f[v_*]/\delta v_*(z)$ in terms of $\sigma_\pm(\mathsf{k})$ and $\delta\eta_\pm(\mathsf{k})$, taking into account that $\delta\sigma_\pm(\mathsf{k})$ and $\delta\eta_\pm(\mathsf{k})$ are related via Kramers-Kronig relations. This gave us integral equations for $\sigma_\pm(k)$, which we managed to solve, obtaining

$$\begin{aligned}
A_+(\mathsf{k}) &= \sqrt{\frac{\mathsf{k}}{\arctan \mathsf{k}}}, \quad \eta_+(\mathsf{k}) = \int_0^\infty \mathrm{d}\mathsf{u}\, \frac{2\arctan(\mathsf{k}\tanh \mathsf{u})}{4\mathsf{u}^2 + \pi^2}, \\
A_-(\mathsf{k}) &= \frac{|\mathsf{k}|}{\sqrt{1 + \pi|\mathsf{k}|/2}}, \\
\eta_-(\mathsf{k}) &= \mathrm{sgn}(\mathsf{k}) \Bigg\{ \frac{\pi}{2} + \frac{1}{2\pi} \Bigg[\mathrm{Li}_2\Big(-\frac{\pi|\mathsf{k}|}{2}\Big) - \mathrm{Li}_2\Big(\frac{\pi|\mathsf{k}|}{2}\Big) \\
&\qquad - \ln\left(\frac{\pi|\mathsf{k}|}{2}\right) \ln\frac{2 - \pi|\mathsf{k}|}{2 + \pi|\mathsf{k}|} \Bigg] \Bigg\}.
\end{aligned}$$

The phase shifts $\eta_\pm(\mathsf{k})$ are plotted in Fig. 4.

These results enabled us to compute the scaling function of the surface two-point function exactly. Since the order parameter varies as $\sqrt{z}$ for $z \to 0$, an appropriate boundary operator that does not vanish at $z = 0$ can be defined by $\Phi_s(\boldsymbol{y}) \equiv \lim_{z\to 0} z^{-1/2}\, \Phi(\boldsymbol{y}, z)$. For its correlation function we obtained

$$\langle \Phi_s(\boldsymbol{y})\, \Phi_s(\boldsymbol{0}) \rangle = \frac{1}{2\pi y^2} \left\{ \theta(m)\, e^{-my} + \theta(-m) \left[1 + |m| y + \frac{m^2 y^2}{2} \right] \right\}, \quad (36)$$

whereas the bulk correlation function is given by

$$\langle \Phi(\boldsymbol{y}, \infty)\, \Phi_(\boldsymbol{0}, \infty) \rangle = \frac{1}{4\pi y} \left\{ e^{-my} \theta(m) + \theta(-m)\, [1 + |m| y] \right\}. \quad (37)$$

Building on the IST results, we were also able to compute the following

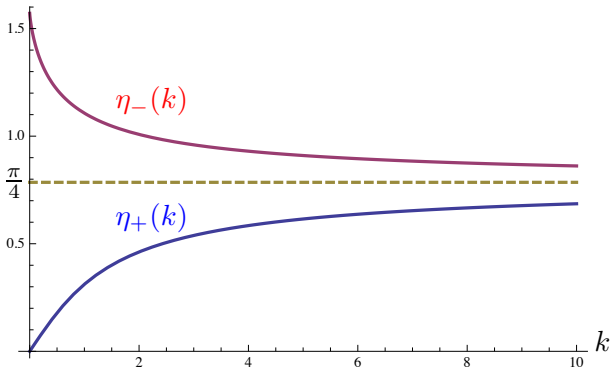

Figure 4: Phase shifts $\eta_-(k)$ for $m=-1$ (red) and $\eta_+(k)$ for $m=+1$ (blue), and $m=0$ (yellow)

modified excess energy density for $m \leq 0$ exactly:

$$\int_0^\infty \mathrm{d}z \left[\langle \Phi(\boldsymbol{y}, z) \rangle^2 - \frac{m^3}{4\pi} \left(1 - \frac{\theta(z|m|-1)}{2z|m|} \right) \right] = -\frac{1+\gamma_\mathrm{E}+\ln(4/\pi)}{2} \frac{m^2}{4\pi}. \tag{38}$$

Here the 1 in the parentheses provides the usual subtraction of the bulk term $\langle \Phi(\boldsymbol{y}, \infty) \rangle^2$. The additional subtraction associated with the term involving $\theta(z|m|-1)$ is necessary at $d=3$ because the energy density has for $d>2$ a power-law tail $\sim z^{-(d-2)}|_{d=3} = 1/z$ due to spin waves [21, 19, 59].

Exact results can also be obtained for properties of the scaling functions $\Theta(x)$ and $\vartheta(x)$. The total free energy for $L<\infty$ is regular at T_c. However, the residual free energy f_res involves subtractions that are nonanalytic at T_c. Therefore, singular terms must appear in the small-x form of its scaling function $\Theta(x)$ that compensate the mentioned nonanalytic terms. These singularities are of the form [47]

$$\Theta(x) - \Delta_\mathrm{C} \underset{x\to 0}{\approx} -\left[\Delta A_0^{(\mathrm{s})} + \frac{x}{48\pi} \right] 2x^2\, \theta(x) + \frac{1}{2\pi^3}\, x^2 \ln|x| + \ldots, \tag{39}$$

where the ellipsis denotes regular terms of linear and higher orders in x, while $\Delta A_0^{(\mathrm{s})}$ is a universal amplitude difference associated with the thermal

singularity of $f_{\rm s}$. The latter is given by [21]

$$\Delta A_0^{(\rm s)} = \int_0^\infty \frac{{\rm d}u}{16\pi}\,\frac{\coth(u)-1/u}{u^2+\pi^2/4} = \frac{1}{2\pi^3}\sum_{\mathsf{k}=1}^{\infty}\frac{\ln(2\mathsf{k})}{4\mathsf{k}^2-1} = 0.00944132199\ldots. \tag{40}$$

As an immediate consequence of Eq. (39), one finds that the second derivative of ϑ has the exact value

$$\vartheta_3''(0) = -\pi^{-3}. \tag{41}$$

It is much harder to work out the asymptotic behavior of $\Theta(x)$ for $x \to -\infty$, namely

$$\Theta(x) \underset{x\to-\infty}{\simeq} -\frac{\zeta(3)}{16\pi}\Big[1+\frac{d_1+2\ln|x|}{|x|}+{\rm o}(|x|^{-1})\Big], \tag{42}$$

with

$$d_1 = 2\left[\gamma_{\rm E}+\ln\frac{4}{\pi}\right]-1-2\frac{\zeta'(3)}{\zeta(3)} = 0.967205644660601\ldots \tag{43}$$

The reason is that the asymptotic behaviors are needed both in the near-boundary and inner regions $z < |m|^{-1} < L/2$ and $|m|^{-1} < z < L$, respectively. This can be done by using distinct semiclassical expansion in either one of them and matching the solutions in the intermediate region [21]. Such a procedure turned out to be necessary, in particular, for the determination of the coefficient d_1. By contrast, the coefficient of the anomalous term $\sim |x|^{-1}\ln|x|$ can also be determined by mapping to a nonlinear σ model [17].

It is also possible to determine the asymptotic behavior of the scaled eigenvalues $\varepsilon_\nu(1,mL) = L^2\,\varepsilon_\nu(L,m)$ in the limit $x \equiv mL \to -\infty$. One finds [21]

$$\varepsilon_\nu(1,x) \underset{x\to-\infty}{=} \begin{cases} \frac{e}{\pi}\,|x|\,e^{-|x|+{\rm o}(1/|x|^0)} & \text{for } \nu=1,\\ \frac{1}{\pi^2(\nu-1)^2}\left[1+\frac{2}{\pi(\nu-1)}\,\frac{\ln(2|x|)}{|x|}+{\rm o}(1/|x|)\right] & \text{for } \nu>1. \end{cases} \tag{44}$$

The leading terms correspond to the spectrum of a free field massless field theory on a strip subject to Neumann boundary conditions [16, 59]. The limit $\Theta(-\infty) = -\frac{\zeta(3)}{16\pi}$ is the associated Casimir amplitude.

5 Concluding remarks

The scaling functions $\Theta(x)$ and $\vartheta(x)$ of the residual free energy and the critical Casimir force in a three-dimensional strip differ qualitatively for prb and fbc. Unlike the case of prb for which exact analytic closed-from expressions for these functions in the limit $n \to \infty$ are known for all values of x, this is not the case for fbc, where one is dependent on numerical means to determine these functions for general values $x \in (-\infty, \infty)$. Nevertheless, a wealth of exact analytic properties of these functions have been derived using a combination of tools such as direct solution of the selfconsistent Schrödinger equation, BOE and SDE, IST methods, mapping to the nonlinear σ model, trace formulae, and matched semiclassical expansions. These exact result have provided helpful benchmarks for assessing the precision of existing and potential future numerical results [16, 17, 48].

6 Acknowledgments

We are grateful to M. Hasenbusch, A. Hucht, and F. Schmidt for fruitful interactions.

References

[1] P. M. Chaikin and T. C. Lubensky. *Principles of condensed matter theory*. Cambridge University Press, Cambridge (GB), 1995.

[2] H. B. G. Casimir. On the attraction between two perfectly conducting plates. *Proc. K. Ned. Akad. Wet.*, B51:793–795, 1948.

[3] E. Buks and M. L. Roukes. Stiction, adhesion energy, and the Casimir effect in micromechanical systems. *Phys. Rev. B*, 63:033402, Jan 2001.

[4] Michael Bordag, Galina Leonidovna Klimchitskaya, Umar Mohideen, and Vladimir Mikhaylovich Mostepanenko. *Advances in the Casimir Effect*. Number 145 in International Series of Monographs on Physics. Oxford University Press, Oxford OX2 6DP, Great Clarendon Street, UK, 2009.

[5] M. E. Fisher and P.-G. de Gennes. Phénomènes aux parois dans un mélange binaire critique. *C. R. Séances. Acad. Sci. Série B*, 287:207–209, 1978.

[6] R. Garcia and M. H. W. Chan. Critical fluctuation-induced thinning of ^{4}He films near the superfluid transition. *Phys. Rev. Lett.*, 83:1187–1190, 1999.

[7] R. Garcia and M. H. W. Chan. Critical Casimir effect near the ^{3}He-^{4}He tricritical point. *Phys. Rev. Lett.*, 88:086101–1–4, 2002.

[8] A. Ganshin, S. Scheidemantel, R. Garcia, and M. H. W. Chan. Critical Casimir force in ^{4}He films: Confirmation of finite-size scaling. *Phys. Rev. Lett.*, 97(7):075301, Aug 2006.

[9] Salima Rafai, Daniel Bonn, and Jacques Meunier. Repulsive and attractive critical Casimir forces. *Physica A*, 386(1):31–35, 2007.

[10] Masafumi Fukuto, Yohko F. Yano, and Peter S. Pershan. Critical Casimir effect in three-dimensional Ising systems: measurements on binary wetting films. *Phys. Rev. Lett.*, 94:135702–1–4, 2005.

[11] C. Hertlein, L. Helden, A. Gambassi, S. Dietrich, and C. Bechinger. Direct measurement of critical Casimir forces. *Nature*, 451:172–175, Jan 2008.

[12] A. Gambassi, A. Maciołek, C. Hertlein, U. Nellen, L. Helden, C. Bechinger, and S. Dietrich. Critical Casimir effect in classical binary liquid mixtures. *Phys. Rev. E*, 80(6):061143, Dec 2009.

[13] Andrea Gambassi. The Casimir effect: From quantum to critical fluctuations. *J. Phys.: Conference Series*, 161(1):012037, 2009.

[14] H. W. Diehl and Felix M Schmidt. The critical Casimir effect in films for generic non-symmetry-breaking boundary conditions. *New Journal of Physics*, 13(12):123025, 2011.

[15] Felix M. Schmidt and H. W. Diehl. Crossover from attractive to repulsive Casimir forces and vice versa. *Phys. Rev. Lett.*, 101(10):100601, 2008.

[16] H. W. Diehl, Daniel Grüneberg, Martin Hasenbusch, Alfred Hucht, Sergei B. Rutkevich, and Felix M. Schmidt. Exact thermodynamic Casimir forces for an interacting three-dimensional model system in film geometry with free surfaces. *EPL (Europhysics Letters)*, 100(1):10004, 2012. arXiv:1205.6613.

[17] H. W. Diehl, Daniel Grüneberg, Martin Hasenbusch, Alfred Hucht, Sergei B. Rutkevich, and Felix M. Schmidt. Large-n approach to thermodynamic Casimir effects in slabs with free surfaces. *Phys. Rev. E*, 89:062123, Jun 2014. arXiv:1405.5787.

[18] Subir Sachdev. *Quantum Phase Transitions*. Cambridge University Press, Cambridge (UK), 2nd edition, 2011.

[19] H. W. Diehl. Field-theoretical approach to critical behaviour at surfaces. In C. Domb and J. L. Lebowitz, editors, *Phase Transitions and Critical Phenomena*, volume 10, pages 75–267. Academic, London, 1986.

[20] H. W. Diehl. The theory of boundary critical phenomena. *Int. J. Mod. Phys. B*, 11:3503–3523, 1997. cond-mat/9610143.

[21] Sergei B. Rutkevich and H. W. Diehl. Inverse-scattering-theory approach to the exact $n \to \infty$ solutions of O(n) ϕ^4 models on films and semi-infinite systems bounded by free surfaces. *Phys. Rev. E*, 91:062114, Jun 2015.

[22] H. W. Diehl and S. Dietrich. Scaling laws and surface exponents from renormalization–group equations. *Phys. Lett.*, 80A:408–412, 1980.

[23] H. W. Diehl and S. Dietrich. Field-theoretical approach to static critical phenomena in semi-infinite systems. *Z. Phys. B: Condens. Matter*, 42:65–86, 1981. Erratum: **43**, 281 (1981).

[24] H. W. Diehl and S. Dietrich. Field-theoretical approach to multicritical behavior near free surfaces. *Phys. Rev. B*, 24(5):2878–2880, Sep 1981.

[25] H. W. Diehl and S. Dietrich. Multicritical behaviour at surfaces. *Z. Phys. B: Condens. Matter*, 50:117–129, 1983.

[26] N. D. Mermin and H. Wagner. Absence of ferromagnetism or antiferromagnetism in one- or two-dimensional isotropic Heisenberg models. *Phys. Rev. Lett.*, 17(2):1133–1136, Nov 1966.

[27] Franz Merkl and Herbert Wagner. Recurrent random walks and the absence of continuous symmetry breaking on graphs. *Journal of Statistical Physics*, 75:153–165, 1994.

[28] Michael E. Fisher, Michael N. Barber, and David Jasnow. Helicity modulus, superfluidity, and scaling in isotropic systems. *Phys. Rev. A*, 8(2):1111–1124, Aug 1973.

[29] A. N. Vasiliev. *Quantum Field Renormalization Group in the Theory of Critical Behavior and Stochastic Dynamics*. PINF Publ., St-Petersburg, 1st edition, 1998. (In Russian). English translation: Aleksandr N. Vasil'ev, The field theoretic renormalization group in critical behavior theory and stochastic dynamics, Chapman and Hall / CRC, 2004.

[30] Moshe Moshe and Jean Zinn-Justin. Quantum field theory in the large N limit: a review. *Phys. Rep.*, 385:69–228, 2003.

[31] Daniel Danchev. Finite-size scaling Casimir force function: Exact spherical-model results. *Phys. Rev. E*, 53:2104–2109, Mar 1996.

[32] Daniel M. Danchev. Exact three-dimensional Casimir force amplitude, c function, and Binder's cumulant ratio: Spherical model results. *Phys. Rev. E*, 58(2):1455–1462, Aug 1998.

[33] Daniel Dantchev, H. W. Diehl, and Daniel Grüneberg. Excess free energy and casimir forces in systems with long-range interactions of van der Waals type: General considerations and exact spherical-model results. *Phys. Rev. E*, 73(1):016131, Jan 2006.

[34] Alfred Hucht. Thermodynamic Casimir effect in ^{4}He films near T_λ: Monte Carlo results. *Phys. Rev. Lett.*, 99(18):185301, 2007.

[35] O. Vasilyev, A. Gambassi, A. Maciołek, and S. Dietrich. Monte Carlo simulation results for critical Casimir forces. *Europhys. Lett.*, 80(6):60009 (6pp), 2007.

[36] O. Vasilyev, A. Gambassi, A. Maciołek, and S. Dietrich. Universal scaling functions of critical Casimir forces obtained by Monte Carlo simulations. *Phys. Rev. E*, 79(4):041142, Apr 2009. Erratum **80**, 039902 (2009).

[37] Martin Hasenbusch. Specific heat, internal energy, and thermodynamic Casimir force in the neighborhood of the λ transition. *Phys. Rev. B*, 81(16):165412, Apr 2010.

[38] Martin Hasenbusch. The specific heat of thin films near the λ-transition: a Monte Carlo study of an improved three-dimensional lattice model. *Journal of Statistical Mechanics: Theory and Experiment*, 2009(10):P10006, 2009.

[39] M. Krech and S. Dietrich. Finite-size scaling for critical films. *Phys. Rev. Lett.*, 66:345–348, 1991. [Erratum **67**, 1055 (1991)].

[40] M. Krech and S. Dietrich. Free energy and specific heat of critical films and surfaces. *Phys. Rev. A*, 46(4):1886–1921, 1992.

[41] H. W. Diehl, Daniel Grüneberg, and M. A. Shpot. Fluctuation-induced forces in periodic slabs: Breakdown of ϵ expansion at the bulk critical point and revised field theory. *Europhys. Lett.*, 75:241–247, June 2006. cond-mat/0605293.

[42] Daniel Grüneberg and H. W. Diehl. Thermodynamic Casimir effects involving interacting field theories with zero modes. *Phys. Rev. B*, 77(11):115409, 2008. arXiv:0710.4436.

[43] H. W. Diehl and Daniel Grüneberg. Critical Casimir amplitudes for n-component ϕ^4 models with $O(n)$-symmetry breaking quadratic boundary terms. *Nucl. Phys. B [FS]*, 822:517–542, 2009.

[44] A. Maciołek, A. Gambassi, and S. Dietrich. Critical Casimir effect in superfluid wetting films. *Physical Review E (Statistical, Nonlinear, and Soft Matter Physics)*, 76(3):031124, 2007.

[45] Roya Zandi, Aviva Shackell, Joseph Rudnick, Mehran Kardar, and Lincoln P. Chayes. Thinning of superfluid films below the critical point. *Physical Review E (Statistical, Nonlinear, and Soft Matter Physics)*, 76(3):030601, 2007.

[46] A. J. Bray and M. A. Moore. Critical behavior of a semi-infinite system: n-vector model in the large-n limit. *Phys. Rev. Lett.*, 38:735–738, Apr 1977.

[47] H. W. Diehl and S. B. Rutkevich. The $O(n)$ ϕ^4 model with free surfaces in the large-n limit: some exact results for boundary critical behaviour, fluctuation-induced forces and distant-wall corrections. *Journal of Physics A: Mathematical and Theoretical*, 47(14):145004, 2014. arXiv:1401.1357.

[48] H. W. Diehl, Daniel Grüneberg, Martin Hasenbusch, Alfred Hucht, Sergei B. Rutkevich, and Felix M. Schmidt. Comment on "Casimir force in the $O(n \to \infty)$ model with free boundary conditions". *Phys. Rev. E*, 91:026101, Feb 2015. arXiv:1405.5787.

[49] Daniel Dantchev, Jonathan Bergknoff, and Joseph Rudnick. Casimir force in the $O(n \to \infty)$ model with free boundary conditions. *Phys. Rev. E*, 89:042116, Apr 2014.

[50] Michael Reed and Barry Simon. *Methods of Modern Mathematical Physics II: Fourier Analysis, Self-Adjointness*. Academic Press, London NW1, Oval Road 24/28 (UK), 1975.

[51] K. M. Case. Singular potentials. *Phys. Rev.*, 80(5):797–806, Dec 1950.

[52] L.D.Landau and E. M. Lifshitz. *Quantum mechanics, non-relativistic theory*, volume 3 of *Course of Theoretical Physics*. Pergamon Press Ltd., London and Paris, 1958.

[53] Klaus Kirsten, Paul Loya, and Jinsung Park. The very unusual properties of the resolvent, heat kernel, and zeta function for the operator $-d^2/dr^2-1/(4r^2)$. *Journal of Mathematical Physics*, 47(4):043506, 2006.

[54] Sergei B. Rutkevich and H. W. Diehl. Inverse scattering theory and trace formulae for one-dimensional Schrödinger problems with singular potentials. *Journal of Physics A: Mathematical and Theoretical*, 48(37):375201, 2015.

[55] William M. Frank, David J. Land, and Richard M. Spector. Singular potentials. *Rev. Mod. Phys.*, 43:36–98, Jan 1971.

[56] John L. Cardy. Universal critical-point amplitudes in parallel-plate geometries. *Phys. Rev. Lett.*, 65:1443–1445, Sep 1990.

[57] D. M. McAvity and H. Osborn. Conformal field theories near a boundary in general dimensions. *Nucl. Phys. B*, 455:522–576, 1995.

[58] H. W. Diehl, S. Dietrich, and E. Eisenriegler. Universality, irrelevant surface operators, and corrections to scaling in systems with free surfaces and defect planes. *Phys. Rev. B*, 27(5):2937–2954, Mar 1983.

[59] H. W. Diehl and A. Nüsser. Critical behavior of the nonlinear σ model with a free surface: The "ordinary" transition in $2+\epsilon$ dimensions. *Phys. Rev. Lett.*, 56(26):2834–2837, Jun 1986.